Electron-phonon coupling in the self-consistent Born approximation of the *t-J* model

O. Gunnarsson and O. Rösch

Max-Planck-Institut für Festkörperforschung, D-70506 Stuttgart, Germany

We study an undoped *t-J* model with electron-phonon interaction using the self-consistent Born approximation (SCBA). By neglecting vertex corrections, the SCBA solves a boson-holon model, where a holon couples to phonons and magnons. Comparison with exact diagonalization results for the *t-J* model suggests that the SCBA describes the electron-phonon interaction fairly accurately over a substantial range of J/t values. Exact diagonalization of the boson-holon model shows that the deviations are mainly due to the neglect of vertex corrections for small J/t and due to the replacement of the *t-J* model by the boson-holon model for large J/t. For typical values of J/t, the electron-phonon part Σ_{ep} of the electron self-energy has comparable contributions from the second-order diagram in the electron-phonon interaction and a phonon-induced change of magnon diagrams. A very simple approximation to Σ_{ep} gives a rather accurate effective mass. Using this approximation, we study the factors influencing the electron-phonon interaction. Typically, we find that the magnons nominally have a stronger coupling to the holon than the phonons. The phonons, nevertheless, drive the formation of small polarons (self-localization) due to important differences between the character of the phonon and magnon couplings.

I. INTRODUCTION

There have recently been several experimental indications that the electron-phonon interaction plays a substantial role for properties of cuprates, for instance in photoemission[1–3] and neutron scattering work.[4] The strong effects of the Coulomb interaction in the cuprates are often taken into account by using the *t-J* model.[5] Including phonons in the *t-J* model, it was concluded that the Coulomb interaction can enhance the effects of the electron-phonon interaction for undoped cuprates.[6,7] It is then interesting to study this aspect further. A simple method for treating the undoped *t-J* model is the self-consistent Born approximation (SCBA),[8–12] which can also be applied to the *t-J* model with phonons.[6,13] This method assumes a quantum Néel ground state for the undoped system. The excitations of the spin system are described by antiferromagnetic magnons. A hole created in, e.g., photoemission is assumed to interact with magnons and phonons, which are both treated as bosons. This model is referred to here as the boson-holon model. The electron self-energy of this model is expressed in terms of the simplest diagrams, including a boson (magnon or phonon) Green's function and a self-consistent electron Green's function. Vertex corrections are neglected.

Here we extend the SCBA study of Ramsak *et al.*,[6] focusing on the limit of weak electron-phonon coupling for $0.2 \leq J/t \leq 2$. For strong electron-phonon coupling, the SCBA is known to break down.[7] We first compare results for the quasiparticle weight and energy using the SCBA and exact diagonalization of the *t-J* model. The results suggest that the SCBA describes the electron-phonon interaction reasonably well for a substantial range of J/t values, but that it is less accurate than for the *t-J* model without phonons. To trace the sources of errors in the SCBA, we use exact diagonalization for the boson-holon model. Comparison between these results and results from the SCBA shows that for small $J/t(\gtrsim 0.2)$, errors in the SCBA are mainly due to the neglect

of vertex corrections in the SCBA, while for large J/t the main source of errors is the replacement of the *t-J* model by the boson-holon model. We then study the electron-phonon contributions to the electron self-energy. There is a contribution from the diagram containing one phonon and one electron Green's function, which for noninteracting electrons is the leading contribution. Here there is a comparable contribution from diagrams containing magnons and one electron Green's function due to the change of the self-consistent electron Green's function induced by the electron-phonon interaction. We also study the effective mass. By slightly modifying a previous approach,[6] we obtain a very simple formula for the effective mass, which agrees rather well with exact results within the SCBA. This formula is used to illustrate the factors influencing the strength of the electron-phonon coupling in the undoped *t-J* model. We discuss the important difference between the coupling to magnons and phonons in terms of strength and effects of vertex corrections. We comment on the implications for formation of small polarons (self-localization).

The boson-holon model and the SCBA are described in Sec. II. The SCBA results are compared with exact diagonalization results for the *t-J* model in Sec. III. In Sec. IV, we compare with exact diagonalization for the holon-boson model to determine the sources of errors in the SCBA. The contributions to the electron-phonon part of the electron self-energy and to the effective mass are discussed in Secs. V and VI, respectively. In Sec. VII, we compare the coupling to magnons and phonons and discuss polaron formation.

II. MODEL AND METHOD

The *t-J* model[5] is given by the Hamiltonian

$$H_{t\text{-}J} = J \sum_{\langle i,j \rangle} \left(\mathbf{S}_i \cdot \mathbf{S}_j - \frac{n_i n_j}{4} \right) - t \sum_{\langle i,j \rangle \sigma} (\tilde{c}_{i\sigma}^\dagger \tilde{c}_{j\sigma} + \text{H.c.}), \quad (1)$$

where $\tilde{c}_{i\sigma}^\dagger$ creates a hole on site i if this site previously had no hole. The Zhang-Rice singlets are represented by empty

174521-1

sites. Here t is a hopping integral, J is the exchange interaction, $\mathbf{S}_i$ is the spin on site $\mathbf{R}_i$, and n_i is the occupation of site i. We use the electron-phonon interaction

$$H_{\rm ep} = \frac{1}{\sqrt{N}} \sum_{i,\mathbf{q}} g_{\mathbf{q}} (n_i - 1)(b_{\mathbf{q}} + b_{-\mathbf{q}}^{\dagger}) e^{i\mathbf{q}\cdot\mathbf{R}_i}, \qquad (2)$$

where N is the number of sites and $b_{\mathbf{q}}^{\dagger}$ creates a phonon with the wave vector $\mathbf{q}$. We assume an on-site coupling with the strength $g_{\mathbf{q}}$. The coupling to hopping integrals and to the spin-spin interaction is neglected. For instance, for the planar (half-)breathing mode in the cuprates it is found that this is a good model.[14] In the following, we assume in addition a Holstein type of coupling, i.e., $g_{\mathbf{q}} \equiv g$ is $\mathbf{q}$-independent.

Following previous work[6,8–12] for the undoped system, the Hamiltonian $H_{t-J} + H_{\rm ep}$ is approximately rewritten in terms of a boson-holon model, where spinless holons interact with phonons and antiferromagnetic magnons, treated as bosons,

$$\widetilde{H} = \frac{1}{\sqrt{N}} \sum_{\mathbf{kq}} [h_{\mathbf{k-q}}^{\dagger} h_{\mathbf{k}} (M_{\mathbf{kq}} a_{\mathbf{q}}^{\dagger} + g_{\mathbf{q}} b_{\mathbf{q}}^{\dagger}) + {\rm H.c.}]$$
$$+ \sum_{\mathbf{q}} (\omega_{\mathbf{q}} a_{\mathbf{q}}^{\dagger} a_{\mathbf{q}} + \omega_{\rm ph} b_{\mathbf{q}}^{\dagger} b_{\mathbf{q}}), \qquad (3)$$

where $h_{\mathbf{k}}^{\dagger}$ and $a_{\mathbf{q}}^{\dagger}$ create spinless holons and antiferromagnetic magnons, respectively. The fermion-magnon coupling is given by

$$M_{\mathbf{kq}} = \sqrt{8}t[\gamma_{\mathbf{k-q}}\sqrt{\nu_{\mathbf{q}}^{-1} + 1} - \gamma_{\mathbf{k}}{\rm sgn}(\gamma_{\mathbf{q}})\sqrt{\nu_{\mathbf{q}}^{-1} - 1}], \qquad (4)$$

where $\gamma_{\mathbf{q}} = (\cos q_x + \cos q_y)/2$ and $\nu_{\mathbf{q}} = (1 - \gamma_{\mathbf{q}}^2)^{1/2}$. The magnon frequency is given by $\omega_{\mathbf{q}} = 2J\nu_{\mathbf{q}}$ and the phonon frequency by $\omega_{\rm ph}$.

The Hamiltonian $\widetilde{H}$ is treated in the self-consistent Born approximation. The electron self-energy is then given by[6,8–12]

$$\Sigma(\mathbf{k},\omega) = \frac{1}{N} \sum_{\mathbf{q}} [M_{\mathbf{kq}}^2 G(\mathbf{k-q},\omega-\omega_{\mathbf{q}}) + g_{\mathbf{q}}^2 G(\mathbf{k-q},\omega-\omega_{\rm ph})], \qquad (5)$$

where $G(\mathbf{k},\omega)$ is the holon Green's function,

$$G(\mathbf{k},\omega) = \frac{1}{\omega - \Sigma(\mathbf{k},\omega)}. \qquad (6)$$

Setting $g_{\mathbf{q}} = 0$, we obtain the corresponding quantities without electron-phonon coupling, $G_0(\mathbf{k},\omega)$ and $\Sigma_0(\mathbf{k},\omega)$. We also introduce the electron-phonon part of the electron self-energy,

$$\Sigma_{\rm ep}(\mathbf{k},\omega) = \Sigma(\mathbf{k},\omega) - \Sigma_0(\mathbf{k},\omega), \qquad (7)$$

and split $\Sigma_{\rm ep}(\mathbf{k},\omega)$ in two contributions,

$$\Sigma_{\rm ep}^{\rm 2nd}(\mathbf{k},\omega) = \frac{1}{N} \sum_{\mathbf{q}} g_{\mathbf{q}}^2 G(\mathbf{k-q},\omega-\omega_{\rm ph}) \qquad (8)$$

and

$$\Sigma_{\rm ep}^{\Delta}(\mathbf{k},\omega) = \frac{1}{N} \sum_{\mathbf{q}} M_{\mathbf{kq}}^2 [G(\mathbf{k-q},\omega-\omega_{\mathbf{q}}) - G_0(\mathbf{k-q},\omega-\omega_{\mathbf{q}})]. \qquad (9)$$

Here $\Sigma_{\rm ep}^{\rm 2nd}(\mathbf{k},\omega)$ corresponds to the second order diagram in the electron-phonon coupling. For noninteracting electrons this is the leading contribution in g^2 to Σ. For the interacting system there is a second contribution of the same order in g, $\Sigma_{\rm ep}^{\Delta}(\mathbf{k},\omega)$. This is due to the change of the contribution from the diagram describing the coupling to magnons caused by the change of the Green's function when the electron-phonon coupling is turned on. We also introduce[6]

$$\Sigma_{\rm ep}^{\rm coh}(\mathbf{k},\omega) = \frac{1}{N} \sum_{\mathbf{q}} g_{\mathbf{q}}^2 G_0^{\rm coh}(\mathbf{k-q},\omega-\omega_{\rm ph}), \qquad (10)$$

where $G_0^{\rm coh}(\mathbf{k-q},\omega-\omega_{\rm ph})$ only includes the coherent part of the Green's function,

$$G_0^{\rm coh}(\mathbf{k},\omega) = \frac{Z_0(\mathbf{k})}{\omega - \varepsilon_0(\mathbf{k})}. \qquad (11)$$

Here $Z_0(\mathbf{k})$ and $\varepsilon_0(\mathbf{k})$ are the quasiparticle strength and energy, respectively, in a system where $g=0$. Since we consider the limit of weak electron-phonon coupling below, we have neglected the effect of the electron-phonon coupling on $Z(\mathbf{k})$ and $\varepsilon(\mathbf{k})$ in Eqs. (10) and (11). The quasiparticle energy is determined by the Dyson equation,

$$\varepsilon_0(\mathbf{k}) = \Sigma_0(\mathbf{k},\varepsilon_0(\mathbf{k})). \qquad (12)$$

The shift of the quasiparticle energy due to the electron-phonon interaction is then

$$\Delta\varepsilon(\mathbf{k}) \equiv \varepsilon(\mathbf{k}) - \varepsilon_0(\mathbf{k}) \approx Z_0(\mathbf{k})\Sigma_{\rm ep}(\mathbf{k},\varepsilon_0(\mathbf{k})), \qquad (13)$$

where

$$Z_0(\mathbf{k}) = \left[1 - \frac{\partial\Sigma_0(\mathbf{k},\omega)}{\partial\omega}\bigg|_{\omega=\varepsilon_0(\mathbf{k})}\right]^{-1}. \qquad (14)$$

III. COMPARISON WITH EXACT DIAGONALIZATION

There have been extensive comparisons of results from the SCBA and exact diagonalization for small clusters for the case of no electron-phonon interaction,[8–12] and the two methods have been found to agree rather well. Here we therefore focus on the changes due to the electron-phonon interaction. We define a dimensionless electron-phonon interaction λ_Z from

$$\frac{Z_0(\pi/2,\pi/2)}{Z(\pi/2,\pi/2)} - 1 \equiv \lambda_Z, \qquad (15)$$

where $Z(\pi/2,\pi/2)$ is the quasiparticle weight for $\mathbf{k} = (\pi/2,\pi/2)$ including the electron-phonon coupling. We study a 4×4 lattice with periodic boundary conditions in the limit of weak electron-phonon coupling, for which exact diagonalization can easily be performed. Following earlier work,[6,7] we define λ_0 as the corresponding quantity for a
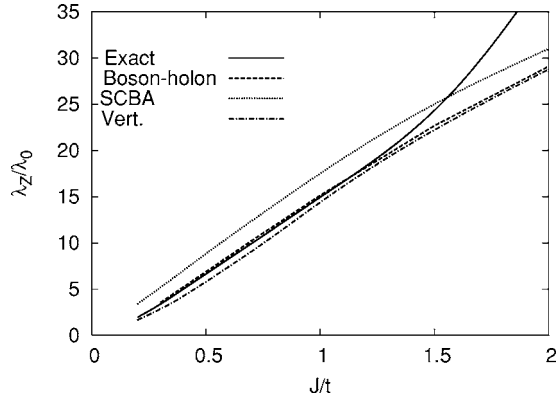
FIG. 1. λ_Z/λ_0 [Eqs. (15) and (16)] for $\omega_{ph}/t=0.1$ as a function of J/t for a 4×4 cluster according to exact diagonalization of the t-J (full line) and the boson-holon (dashed line) models, the SCBA (dotted line) and SCBA together with the lowest-order vertex corrections (dash-dotted line) in the limit of a small coupling g.

FIG. 2. Energy shift $\Delta\varepsilon$ for $\mathbf{k}=(\pi/2, \pi/2)$ [Eq. (13)] for a 4 $\times 4$ cluster with $\omega_{ph}/t=0.1$ according to exact diagonalization of the t-J (full line) and the boson-holon (dashed line) models, the SCBA (dotted line) and SCBA together with the lowest-order vertex corrections (dash-dotted line) in the limit of a small coupling g.

single electron at the bottom of the band of a two-dimensional Holstein model with nearest-neighbor hopping. Assuming $\omega_{ph}/t \ll 1$ and using a quadratic expansion of the band, we obtain

$$\lambda_0 = \frac{g^2}{4\pi t \omega_{ph}}. \qquad (16)$$

The calculations are done for small enough g that the ratio λ_Z/λ_0 is converged to the $g \to 0$ limit. We emphasize that by considering the bottom of the band, the resulting λ_0 is particularly small.[15] At larger filling the corresponding λ_0 is larger and the resulting enhancement of λ_Z is smaller. It is necessary to pay some extra attention to the $\mathbf{q}=\mathbf{0}$ coupling, g_0. By using Eqs. (10), (11), and (13), we find that in the SCBA this component gives a contribution

$$\frac{1}{N}\left(\frac{g_0}{\omega_{ph}}\right)^2 Z_0(\mathbf{k})^2 \qquad (17)$$

to λ_Z. The $\mathbf{q}=\mathbf{0}$ component just couples to the total number of electrons. Since the Green's function describes the addition or removal of an electron, we can alternatively calculate the exact spectrum for one electron coupling to the $\mathbf{q}=\mathbf{0}$ component and then convolute this spectrum with the spectrum resulting from the coupling to the $\mathbf{q} \neq \mathbf{0}$ components. The exact $\mathbf{q}=\mathbf{0}$ contribution to λ_Z is then

$$\frac{1}{N}\left(\frac{g_0}{\omega_{ph}}\right)^2. \qquad (18)$$

This differs from Eq. (17) by a factor of $Z_0(\mathbf{k})^2$, which is typically a very large difference. Although the comparison with exact diagonalization can only be done for a small cluster, we are primarily interested in infinite systems where the $\mathbf{q}=\mathbf{0}$ component plays no role. In discussing λ_Z and $\Delta\varepsilon$ below, we therefore exclude the $\mathbf{q}=\mathbf{0}$ coupling.

Figure 1 shows exact results (full line) and results from the SCBA (dotted line) for $\omega_{ph}/t=0.1$. The dashed and dash-dotted curve are discussed in Sec. IV. The results agree qualitatively. However, quantitatively the agreement is not as
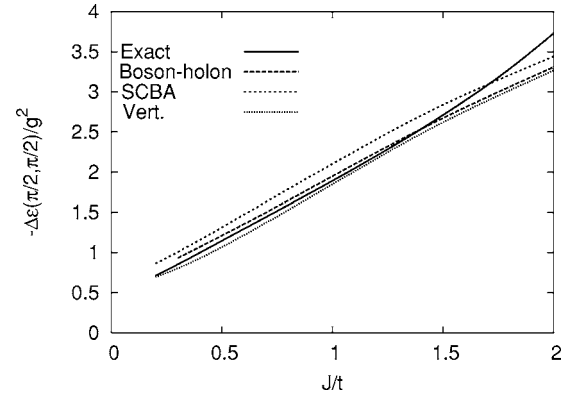
good as found for the model without electron-phonon interaction. This is, in particular, the case for small J/t, which are values usually assigned to the high-T_c cuprates, and for large values of J/t. For instance, λ_Z/λ_0 is about 3.3 and 5.2 according to the exact calculation and the SCBA, respectively, for $J/t=0.3$. Figure 2 shows the energy shift $\Delta\varepsilon(\pi/2, \pi/2)$ [Eq. (13)] due to the electron-phonon interaction for a 4 $\times 4$ cluster. As in the case of λ_Z, the SCBA deviates appreciably from the exact results for small and large values of J/t. The reason for these deviations is discussed in Sec. IV. The agreement with exact results is still good enough to suggest that we can use the SCBA for a qualitative discussion of properties of the t-J model with phonons.

IV. ACCURACY OF APPROXIMATIONS BEHIND THE SCBA

In view of the results in Figs. 1 and 2, it is interesting to ask for the sources of errors in the SCBA. We distinguish between two classes of errors: (i) the replacement of the t-J model in Eq. (1) by the boson-holon model in Eq. (3) and (ii) the neglect of vertex corrections when solving this model.

We consider the first class of errors by solving the boson-holon model [Eq. (3)] using exact diagonalization in the limit of weak electron-phonon coupling. The Hilbert space can then be limited by only considering states with at most one phonon excited. Due to the strong holon-magnon coupling, however, it is necessary to consider states with many excited magnons. Figures 1 and 2 compare these results with results from diagonalizing the t-J model. Except for large J/t, the agreement is very good. This shows that for small and intermediate values of J/t, the errors in the SCBA are mainly due to vertex corrections, while for large J/t the replacement of the t-J model by the boson-holon model leads to appreciable errors.

We next consider vertex corrections. Figure 3(a) shows a second-order diagram that is not included in the SCBA, due to the crossing magnon lines and resulting vertex correction.
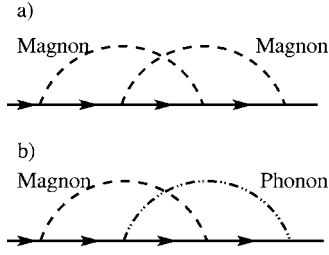
FIG. 3. Self-energy diagrams including (a) two crossing magnon lines and (b) crossing magnon and phonon lines. The magnon, phonon, and self-consistent electron propagators are represented by dashed, dash-dotted, and full lines, respectively.

It was shown by Liu and Manousakis[12] that this diagram and many other diagrams neglected in the SCBA are actually zero due to the symmetry of $M_{\mathbf{kq}}$. This makes it understandable why the neglect of vertex corrections is found to be a rather good approximation for magnons.

In the limit of weak electron-phonon coupling discussed in this paper, diagrams with crossing phonon lines do not contribute to lowest order in $g_{\mathbf{q}}^2$. Diagrams involving magnon line(s) crossing one phonon line, however, do contribute to this order in $g_{\mathbf{q}}^2$. Figure 3(b) shows the lowest order diagram of this type. In contrast to the pure magnon diagram in Fig. 3(a), the diagram in Fig. 3(b) is in general not zero. We have included this diagram and an equivalent diagram in the calculations, using self-consistent propagators for all electron lines in the calculation of λ_Z and $\Delta\varepsilon$. The results are shown in Figs. 1 and 2 by the dash-dotted lines. For small J/t, the correction to the SCBA (dashed curve) is large (almost a factor of 2) and it goes in the correct direction compared with the exact result for boson-holon (dashed line) and t-J models (full curve). Some higher-order diagrams are not small, although the sums of all higher-order diagrams apparently almost cancel. The rapid convergence for small J/t suggested by Figs. 1 and 2 is therefore somewhat misleading. We note that these lowest order vertex corrections have a substantially smaller effect on the self-energy for larger clusters. In these cases, however, it is not possible to perform exact diagonalization calculations, and it is therefore not clear if the SCBA becomes more accurate for large clusters.

We observe that diagrams of the type in Fig. 3(b) were neglected in the calculation of the criterion for polaron formation.[7] If the results in Figs. 1 and 2 can be extrapolated to large clusters and strong coupling, they suggest that the earlier criterion[7] for polaron formation may have underestimated the critical λ.

V. QUASIPARTICLE ENERGY

In the remainder of the paper, we focus on the SCBA and first analyze the quasiparticle energies. We have performed calculations for 96×96 lattices, using $t=1$, $J/t=0.3$, $g/t=0.05$, and $\omega_{\mathrm{ph}}/t=0.1$. The self-energy was broadened by adding a small imaginary part $\delta/t=0.005-0.01$ to the energy. Figure 4 compares results for $\Delta\varepsilon(\mathbf{k})$ (full line), determined from the Dyson equation using the full self-energy, with $Z_0(\mathbf{k})\Sigma_{\mathrm{ep}}(\mathbf{k},\varepsilon_0(\mathbf{k}))$ [Eq. (13)] using three approxima-
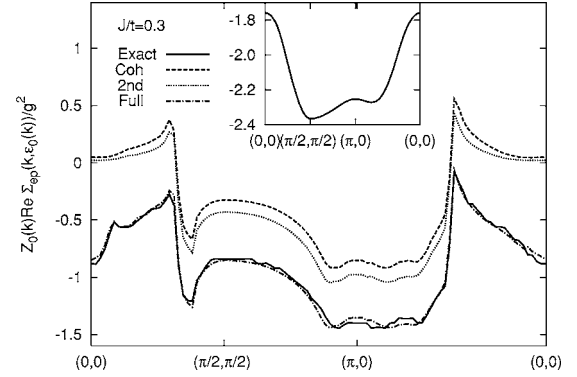

FIG. 4. $Z_0(\mathbf{k})\Sigma_{\mathrm{ep}}(\mathbf{k},\varepsilon_0(\mathbf{k}))$ as a function of $\mathbf{k}$ along the $(0,0)-(\pi/2,\pi/2)$, $(\pi/2,\pi/2)-(0,\pi)$, and $(0,\pi)-(0,0)$ directions. Results are shown for $\Sigma_{\mathrm{ep}}^{\mathrm{coh}}$ [Eq. (10)] (dashed line), $\Sigma_{\mathrm{ep}}^{\mathrm{2nd}}$ [Eq. (8)] (dotted line), and Σ_{ep} [Eq. (7)] (dash-dotted line) as well as for the exact $\Delta\varepsilon(\mathbf{k})$ (full line). The inset shows the dispersion of $\varepsilon_0(\mathbf{k})$. The parameters are $t=1$, $J/t=0.3$, $g/t=0.05$, and $\omega_{\mathrm{ph}}/t=0.1$.

tions for the self-energy. The figure illustrates that $\Sigma_{\mathrm{ep}}^{\mathrm{coh}}$ (dashed line) is a rather good approximation to $\Sigma_{\mathrm{ep}}^{\mathrm{2nd}}$ (dotted line), i.e., the incoherent part of G_0 included in $\Sigma_{\mathrm{ep}}^{\mathrm{2nd}}$ does not contribute much to the self-energy. It is interesting, however, that $\Sigma_{\mathrm{ep}}^{\mathrm{2nd}}$ (dotted line) is a rather poor approximation to Σ_{ep} (dash-dotted line), and it only contributes about half the magnitude for $J/t=0.3$. Both $\Sigma_{\mathrm{ep}}^{\mathrm{2nd}}$ and $\Sigma_{\mathrm{ep}}^{\Delta}$ are of the order $g_{\mathbf{q}}^2$. For large values of J/t, this difference is smaller. For noninteracting electrons, Σ_{ep} is the only contribution of this order, and the interest has therefore often focused on this contribution. Figure 4 shows that this is not a good approximation for the present model and $J/t=0.3$. The full line and the dash-dotted line differ slightly since the solution in Eq. (13) of the Dyson equation is only approximate for a finite g.

To better understand the results for $\Sigma_{\mathrm{ep}}^{\mathrm{2nd}}$, we notice that for a $\mathbf{q}$-independent $g_{\mathbf{q}}\equiv g$, Im$\Sigma_{\mathrm{ep}}^{\mathrm{2nd}}$ takes a very simple form,

$$\mathrm{Im}\Sigma_{\mathrm{ep}}^{\mathrm{2nd}}(\mathbf{k},\omega) = \pi g^2 A(\omega - \omega_{\mathrm{ph}}), \qquad (19)$$

where $A(\omega) = \Sigma_{\mathbf{k}}\mathrm{Im}G_0(\mathbf{k},\omega-i0^+)/(N\pi)$ is the $\mathbf{k}$-averaged spectral function. Figure 5 shows $A(\omega)$. Since we used
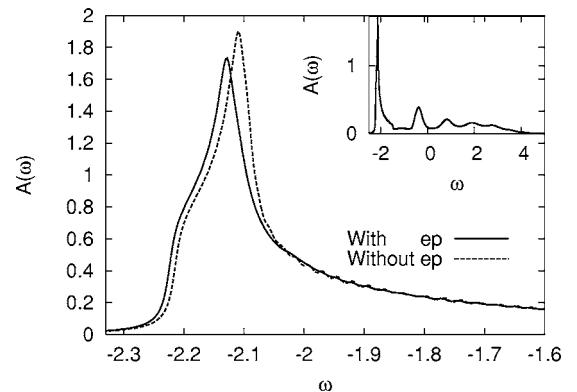

FIG. 5. Spectral function $A(\omega)$ with (full line) and without (dashed line) electron-phonon coupling. The parameters are the same as in Fig. 4, except $g=0.1t$. A Lorentzian broadening with FWHM $0.2t$ was used.

$\omega_{ph}/t=0.1$ in Fig. 4, the onset of $\text{Im}\Sigma_{ep}$ has been shifted by $0.1t$ above the bottom of the band. States below this onset are then shifted strongly downwards, while states above the onset are shifted less or are even shifted upwards. From the inset of Fig. 4, we can see that states around $(\pi/2,\pi/2)$ and along the line $(\pi/2,\pi/2)-(\pi,0)$ are below the onset and are shifted strongly downwards, in particular states that are just below the onset, while Σ_{ep}^{2nd} becomes positive for **k** vectors along the lines $(0,0)-(\pi/2,\pi/2)$ and $(\pi,0)-(0,0)$ close to $(0,0)$.

In a similar way, we can understand Σ_{ep}^{Δ} [Eq. (9)], although in this case the coupling $M_{\mathbf{kq}}$ and the energy $\omega_{\mathbf{q}}$ have strong **k** and **q** dependences. Σ_{ep}^{Δ} is due to the coupling to the changes of $A(\mathbf{k},\omega)$ caused by the electron-phonon coupling. Figure 5 shows the **k**-average $A(\omega)$ with (full line) and without (dashed line) electron-phonon coupling. The parameters are the same as for Fig. 4, except that $g/t=0.1$ to enhance the effect of the electron-phonon coupling. This difference in $A(\omega)$ is positive and particularly large at $\omega\approx-2.2$. Since $\omega_{\mathbf{q}}$ can be fairly large, ranging from zero to $2J=0.6t$, $\text{Im}\Sigma_{ep}^{\Delta}$ is shifted substantially upwards in frequency. As a result, $\text{Re}\Sigma_{ep}^{\Delta}$ is negative for the whole quasiparticle band.

VI. EFFECTIVE MASS

We next consider the effective mass, essentially following Ramsak *et al.*[6] Since Σ_{ep}^{Δ} is relatively **k**-independent, we neglect it and we only consider Σ_{ep}^{coh}. For simplicity, we assume that $Z_0(\mathbf{k})=Z_0(\pi/2,\pi/2)$ is **k**-independent. We furthermore approximate the quasiparticle dispersion by assuming that it can be expanded quadratically around the four minima $(\pm\pi/2,\pm\pi/2)$. Two masses are introduced, $m_{\parallel}$ and $m_{\perp}$, which describe the dispersion parallel and perpendicular to the $(0,0)-(\pi,\pi)$ direction, respectively. The summation over the Brillouin zone in Eq. (10) is replaced by an integration over all of **q** space, assuming that contributions far away from $(\pm\pi/2,\pm\pi/2)$ are small because of the large energy denominator in Eqs. (10) and (11). By using the solution of the Dyson equation (13), we then obtain

$$\Delta\varepsilon(\mathbf{k}) = 4\left(\frac{1}{2\pi}\right)^2 \int d^2q \frac{g^2 Z_0^2}{\varepsilon_0(\mathbf{k})-\varepsilon_0(\mathbf{k}-\mathbf{q})-\omega_{ph}}, \quad (20)$$

where the factor 4 is due to the presence of four equivalent minima $(\pm\pi/2,\pm\pi/2)$. One factor of Z_0 comes from the Green's function and a second factor from solving the Dyson equation. Defining the effective mass along the parallel direction as $1/m^*=d^2\varepsilon(\mathbf{k})/dk_{\parallel}^2$, we obtain

$$\frac{m_{\parallel}}{m^*} - 1 = -\frac{2g^2 Z_0^2\sqrt{m_{\parallel}m_{\perp}}}{\pi\omega_{ph}} \equiv \left(\frac{1}{1+\lambda_m}-1\right), \quad (21)$$

where the second equality defines the electron-phonon coupling λ_m. Focusing on large J/t, Ramsak *et al.*[6] obtained the same result except for a factor Z_0 resulting from the Dyson equation (13). Without this factor, the rather good agreement with the exact result in Fig. 6 would be lost for small J/t. λ_m is compared with the corresponding quantity for the Holstein model,[6] which is identical to the λ_0 defined via Z in Eq. (16).

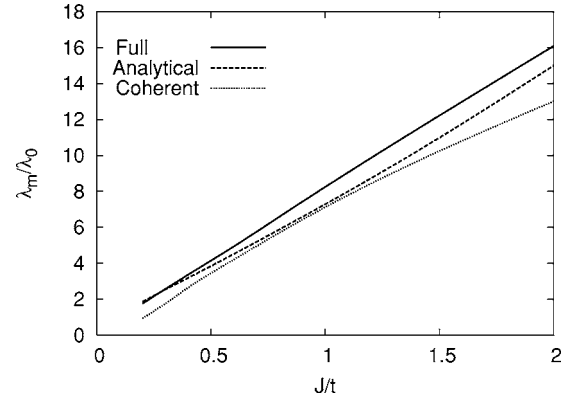FIG. 6. λ_m/λ_0 as a function of J/t calculated from the quasiparticle energy $\varepsilon(\mathbf{k})$ (full line), Eq. (21) (dashed line), and using the self-energy Σ_{ep}^{coh} [Eq. (10)]. The parameters are the same as in Fig. 4, except that $g=0.1t$ and J/t is varied.

Figure 6 shows results for λ_m/λ_0 as a function of J/t, using the second derivative of the exact $\varepsilon(\mathbf{k})$ (full line) and of $\varepsilon(\mathbf{k})$ obtained from Σ_{el}^{coh} (dotted line) as well as Eq. (21) (dashed line). λ_m/λ_0 is different from λ_Z/λ_0 in Fig. 1. The main reason for this difference is that Fig. 1 shows results for a 4×4 cluster while Fig. 6 shows results for a large cluster $(96\times96$ or $128\times128)$, but the two quantities are somewhat different also for identical clusters. The results based on Σ_{el}^{coh} (dotted line) agree rather well with the exact results for intermediate and large values of J/t, while they are too small for small values of J/t. The deviation for small J/t is primarily due to the neglect of Σ_{ep}^{Δ}. This term is particularly important for small J/t, since the magnon energy entering in Eq. (9) is proportional to J. For large J/t, the deviation is mainly due to the neglect of the incoherent part of G. Equation (21) (dashed curve), which is an approximation to the dotted curve, gives a larger λ_m and it agrees better with the exact result. For small J/t, the increase is primarily due to neglect of **k** dependence of $Z_0(\mathbf{k})$ in the Dyson equation when deriving Eq. (21). For large J/t, the increase is due to several small errors in the approximations. The coupling $g/t=0.1$ is somewhat too large to give the weak-coupling limit, in particular for large J/t.

We are now in the position to interpret the enhancement of λ_m compared with λ_0 obtained at the bottom of the band for a Holstein model. Equation (21) contains a factor Z_0^2 that tends to reduce the coupling due to the transfer of spectral weight far away from the energies studied. On the other hand, the factor $\sqrt{m_{\parallel}m_{\perp}}$ describes how the energy denominator is reduced by the large effective masses, bringing spectral weight closer to the relevant energies.[6] This is an effect of correlation and antiferromagnetism, and it is important for the enhancement of the electron-phonon interaction in this model. In addition, there is a factor of 4 resulting from the presence of the four equivalent minima $(\pm\pi/2,\pm\pi/2)$. For $J/t=0.2$, we find that $Z_0^2=0.05$ and $\sqrt{m_{\parallel}m_{\perp}}=10m_0$, where $m_0=1/(2t)$ is the mass at the bottom of the band in the Holstein model. In this case, the factor 4 from the equivalent minima is crucial, since the electron-phonon interaction would otherwise have been suppressed in the t-J model, while now it is enhanced by a factor of 1.8. For $J/t=2$, we

obtain $Z_0^2 = 0.57$ and $\sqrt{m_\parallel m_\perp} = 6.5 m_0$, giving the enhancement 16 [15 according to Eq. (21)]. In this case, the large mass plays a crucial role for the enhancement of the electron-phonon interaction. We notice, however, that the comparison here has been done with λ_0 calculated for a single electron at the bottom of the band of a Holstein model. Had the comparison been made with a half-filled Holstein model, the result would have been a smaller enhancement or no enhancement at all.[15] By starting from the three-band model and studying the half-breathing phonon, however, it is found that the coupling constants $g_\mathbf{q}$ are enhanced by correlation effects.[16]

VII. COMPARISON OF COUPLING TO MAGNONS AND PHONONS

We define an average dimensionless coupling constant for the magnons,

$$\lambda_M \equiv \frac{1}{N} \sum_\mathbf{k} \lambda_{M\mathbf{k}} = \frac{1}{N^2} \sum_{\mathbf{qk}} \frac{2M_{\mathbf{kq}}^2}{8t\omega_\mathbf{q}} = \frac{t}{2J}, \quad (22)$$

where $\lambda_{M(\pi/2,\pi/2)} = 0.65t/J$. For La_2CuO_4, the corresponding quantity due to phonons is $\lambda = 1.2$.[17] For a typical value $J/t = 0.3$,[18] the coupling to magnons, $\lambda_M = 1.67$ and $\lambda_{M(\pi/2,\pi/2)} = 2.2$, is stronger than the coupling to phonons. It might then seem that the coupling to magnons is more important for the experimentally observed[2] polaron formation in undoped cuprates. This is, however, misleading. The value of λ needed for formation of small polarons is reduced with the boson frequency.[19–21] This somewhat favors phonons, since they typically have lower frequencies than the magnon frequencies of the order of J. To see the main difference, however, it is necessary to consider vertex corrections.

To describe the formation of small polarons due to phonons, it is crucial to go beyond the SCBA, since vertex corrections including phonon propagators become very important in the strong-coupling limit.[7] Actually, if these vertex corrections are neglected, polaron formation is not properly obtained.[7] On the other hand, it has been argued that vertex corrections including magnon propagators are not very important in the t-J model.[8,9,11,12] As discussed in Sec. IV, the lowest-order vertex correction in Fig. 3(a) is identically zero due to the symmetry of $M_{\mathbf{kq}}$, and classes of higher-order vertex corrections are also zero.[12] If we assume a Holstein type of electron-phonon coupling, however, there are no similar arguments for diagrams with crossing phonon lines being zero. This explains why the holon-phonon interaction, but not the holon-magnon interaction, leads to polaron formation.

VIII. SUMMARY

To summarize, we have studied the self-consistent Born approximation (SCBA) in the limit of weak electron-phonon coupling. While the SCBA has been shown to be quite accurate for a pure t-J model, we find that it is less accurate when the electron-phonon interaction is included. To study the reason for this, we performed exact diagonalization calculations for the boson-holon model. Comparing the results with the SCBA results, we find that the main errors of the SCBA are due to the neglect of vertex corrections for small J/t and due to the introduction of the boson-holon model itself for large J/t. Studying the electron-phonon part of the self-energy, we find that in addition to the second-order term Σ_{ep}^{2nd} known from the theory of noninteracting electrons, there is a second term of the same order, Σ_{ep}^Δ. For $J/t \approx 0.3$, this term makes a similar contribution to Σ_{ep} as Σ_{ep}^{2nd}. We have shown that a very simple derivation of the effective mass gives a rather accurate result, illustrating the factors enhancing and suppressing the electron-phonon coupling. The coupling to magnons can be considered stronger than the coupling to phonons for realistic parameters. Nevertheless, the phonons drive the formation of small polarons for undoped cuprates, due to the difference between phonons and magnons, in particular the different importance of vertex corrections.

[1] A. Lanzara *et al.*, Nature (London) **412**, 510 (2001).

[2] K. M. Shen *et al.*, Phys. Rev. Lett. **93**, 267002 (2004).

[3] G.-H. Gweon, T. Sasagawa, S. Y. Zhou, J. Graf, H. Takagi, D.-H. Lee, and A. Lanzara, Nature (London) **430**, 187 (2004).

[4] L. Pintschovius, Phys. Status Solidi B **242**, 30 (2005).

[5] F. C. Zhang and T. M. Rice, Phys. Rev. B **37**, 3759 (1988).

[6] A. Ramsak, P. Horsch, and P. Fulde, Phys. Rev. B **46**, 14305 (1992).

[7] A. S. Mishchenko and N. Nagaosa, Phys. Rev. Lett. **93**, 036402 (2004).

[8] S. Schmitt-Rink, C. M. Varma, and A. E. Ruckenstein, Phys. Rev. Lett. **60**, 2793 (1988).

[9] C. L. Kane, P. A. Lee, and N. Read, Phys. Rev. B **39**, 6880 (1989).

[10] F. Marsiglio, A. E. Ruckenstein, S. Schmitt-Rink, and C. M. Varma, Phys. Rev. B **43**, 10882 (1991).

[11] G. Martinez and P. Horsch, Phys. Rev. B **44**, 317 (1991).

[12] Z. Liu and E. Manousakis, Phys. Rev. B **45**, 2425 (1992).

[13] B. Kyung, S. I. Mukhin, V. N. Kostur, and R. A. Ferrell, Phys. Rev. B **54**, 13167 (1996).

[14] O. Rösch and O. Gunnarsson, Phys. Rev. Lett. **92**, 146403 (2004).

[15] G. Sangiovanni, O. Gunnarsson, E. Koch, C. Castellani, and M. Capone, cond-mat/0602606 (unpublished).

[16] O. Rösch and O. Gunnarsson, Phys. Rev. B **70**, 224518 (2004).

[17] O. Rösch, O. Gunnarsson, X. J. Zhou, T. Yoshida, T. Sasagawa, A. Fujimori, Z. Hussain, Z.-X. Shen, and S. Uchida, Phys. Rev. Lett. **95**, 227002 (2005).

[18] J. Jaklic and P. Prelovsek, Adv. Phys. **49**, 1 (2000).

[19] H. Fehske, J. Loos, and G. Wellein, Z. Phys. B: Condens. Matter **104**, 619 (1997).

[20] S. Ciuchi, F. de Pasquale, S. Fratini, and D. Feinberg, Phys. Rev. B **56**, 4494 (1997).

[21] A. S. Alexandrov and P. E. Kornilovitch, Phys. Rev. Lett. **82**, 807 (1999).